A Compact Tri-Band Bandpass Filter with Independently Controllable Harmonic Bandwidth by Using Two Grounded Vias

Peng Wang, Xiang An[*], and Zhi-Qing Lv

Abstract—A new class of tri-band bandpass filter(BPF) is presented, and harmonic passband bandwidth can be independently controlled. In the implementation, three coupling paths are used to control the bandwidth of each passband. The first coupling path is two grounded vias which are utilized to realize coupling between two short-stub loaded resonators. And the first coupling path delivers signals at the first passband. Meanwhile, the second coupling path delivers signals at both the first and second passbands. And the third coupling path only delivers signals at the third passband. Using this method, both the frequency and bandwidth of each passband can be designed and tuned easily. In this filter design, the first harmonic passband can be adjusted separately and is independent of the fundamental passband. Two grounded vias improve flexibility and form a fundamental passband and harmonic passband independently controllable passband filter. For demonstration, a tri-band BPF with three passbands at 1.5 GHz, 2.5 GHz, and 3.5 GHz with insertion losses of 0.34, 0.76 and 1.08 dB is designed, fabricated and measured. So this proposed filter will be attractive in wireless communication systems.

1. INTRODUCTION

In modern wireless communication systems, microwave passband filters (BPF) are very useful and of importance in practice. Due to modern manufacturing technology, microwave planar BPFs have been widely studied and employed. In the past, many methods of designing BPFs have been explored and reported, such as [1–12]. In [1, 2], three sets of resonators were used to design tri-band BPFs due to the use of combining networks. It has the advantage of independent control of passband locations and bandwidths. In [3, 4], two multi-mode resonators were used to design passband filters. The main advantage of these multi-mode resonators is that degenerated modes are independent of each other.

In [5–11], some types of tri-band resonators, such as step-impedance resonator (SIR), stub-loaded resonator (SLR), and stub-loaded step-impedance resonator (SLSIR), were proposed to realize tri-band responses. In [5], grounded stepped impedance resonators and coupled lines were combined to design tri-band BPFs. In [6], asymmetrically loaded resonators with open-ended and short-ended stubs were used to design tri-band BPFs. In [7], an open and short stubs loaded crossed resonator was used to design tri-band BPFs. In [8], a T-shaped stub loaded resonator was used to design tri-band BPFs. In [9], two asymmetric half-wavelength SIRs with tunable coupling structures were used to design tri-band BPFs. In [10], a three-section SIR using parallel coupling structure was used to design tri-band BPFs. In [11, 12], two stub-loaded SIRs were used to design tri-band BPFs. All these tri-band filters make use of the harmonic property of microwave resonators. Although passband frequencies can be adjusted to desirable values, it is not easy to control the bandwidths independently due to the dependence of harmonic wave. To solve this problem, this paper proposes a new way to improve the flexibility to independently adjust harmonic passband bandwidths.

In this paper, a tri-band BPF with controllable harmonic bandwidth is proposed. The filter is designed with combined use of two short-stub loaded resonators and two quarter wavelength uniform impedance resonators (UIRs). Short-stub loaded resonators can produce fundamental passband and the first harmonic passband. The fundamental passband is used for the first passband, and the first harmonic passband is used for the second passband. UIRs are designed to obtain the third resonant frequency. In the implementation, we make use of three coupling paths to control the bandwidth of each passband. The first coupling path and third coupling one independently deliver signals at the first and third passbands, respectively. Meanwhile, the second coupling path delivers signals at both the first and second passbands. By using two coupling paths, i.e., *path1* and *path2*, fundamental passband bandwidth and the first harmonic passband bandwidth can be adjusted separately. It improves flexibility to independently adjust harmonic passband bandwidths. Experimental results show a good agreement with the simulated one. To verify the proposed concept, a tri-band BPF with three passbands at 1.5 GHz, 2.5 GHz, and 3.5 GHz is designed, fabricated and measured. The measured results agree well with the simulated ones.

2. DESIGN PROCEDURE

2.1. Resonance Properties

2.1.1. Short-Stub Loaded Resonator

A short-stub loaded resonator is illustrated in Fig. 1, in which Y_1 and Y_2 are characteristic admittances of the resonator and stub, respectively. According to [13], input admittance of the resonator can be expressed as

$$Y_{in} = jY \frac{-\cot\theta_3 + \tan\theta_2 + \tan\theta_1}{1 + (\cot\theta_3 - \tan\theta_2)\tan\theta_1} \tag{1}$$

where $Y_1 = Y_2 = Y$ is assumed for simplicity. The resonance condition is given by

$$\tan\theta_1 + \tan\theta_2 - \cot\theta_3 = 0 \tag{2}$$
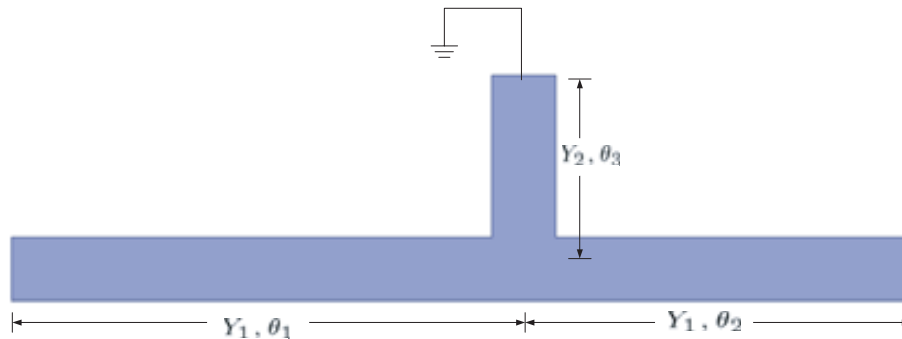
Figure 1. Illustration of the short-stub loaded resonator.

Suppose that the fundamental resonant frequency is f_1 and that the first harmonic resonant frequency is f_2. According to Eq. (2), we can obtain resonant frequencies (f_1, f_2) from given electrical lengths $(\theta_1, \theta_2, \theta_3)$, as shown in Fig. 2, in which, for the sake of clarity, here θ_1 is assumed to be 78°; $k_1 = f_1/f$ and $k_2 = f_2/f$ are normalized frequencies, and f is chosen as 1.76 GHz in this paper. θ_1, θ_2 and θ_3 are the corresponding electrical lengths at f.

2.1.2. Uniform Impedance Resonator (UIR)

Two quarter-wavelength uniform impedance resonators are employed to achieve the third passband, and at resonant frequency f_3, the resonant condition is given by

$$L_{12} = \lambda_3/4 \tag{3}$$

where λ_3 is the guided wavelength at the operating frequency f_3.
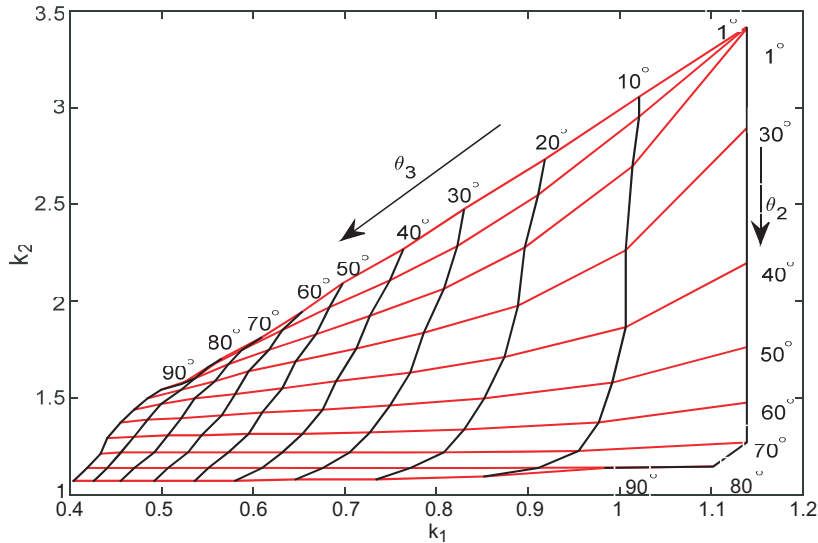
Figure 2. Relation between the electrical lengths $(\theta_1, \theta_2, \theta_3)$ and the resonant frequencies (f_1, f_2). Note θ_1 is assumed to be 78° for clarity.

2.2. Resonator Coupling

The layout of the presented tri-band BPF is shown in Fig. 3. It consists of two types of resonators. Both *Resonator 1* and *Resonator 2* are meandering models of short-stub loaded resonators shown in Fig. 1, and they are connected with two grounded vias. Both *resonator 3* and *resonator 4* are quarter-wavelength winding uniform impedance resonators. They wrap the two short-stub loaded resonators and connect each other with a grounded via. Two feed lines are embedded between the short-stub loaded resonators and the quarter-wavelength uniform impedance resonators. Each feed line is a combination of a conventional tap coupled-line and a parallel coupled-line.

There are three coupling paths in Fig. 3. Two grounded vias are employed to realize the inter-stage coupling between *Resonator 1* and *Resonator 2*, and form a coupling path denoted by *path1* (see Fig. 3). The second coupling path, namely *path2*, is located at the top open ends of the short-stub loaded resonators, as illustrated in Fig. 3. The third coupling path, i.e., *path3*, is generated by a via hole between the two quarter-wavelength uniform impedance resonators, as demonstrated in Fig. 3. The couplings of *path1* and *path3* both can be considered as magnetic couplings, while the coupling of *path2* can be modeled as a electric coupling.

The coupling of *path1* can be tuned by diameter D_1 of two grounded vias (see Fig. 3) and the distance S between the two vias. The coupling in *path2* can be affected by gap g_1 and length of the parallel line, i.e., (see Fig. 3). And the coupling in *path3* can be affected by diameter D_2.

We next present the relations between the coupling paths and bandwidths of each passband by using a full-wave electromagnetic simulation method. In each simulation, only one parameter is changeable. Simulated results are shown in Fig. 4, Fig. 5, Fig. 6, and Fig. 7.

2.2.1. The Coupling of Path1

Bandwidth of the first passband will increase when increasing distance S and diameter D_1, whereas bandwidths of the harmonic passband and the third passband both are unchanged, as shown in Fig. 4 and Fig. 5. This is because the coupling in *path1* will be stronger if S and/or D_1 increase.

2.2.2. The Coupling of Path2

As can be seen from Fig. 6, as gap is changed, both bandwidths of the first passband and harmonic passband can be adjusted. This is because when g_1 decreases, the coupling in *path2* will increase significantly.
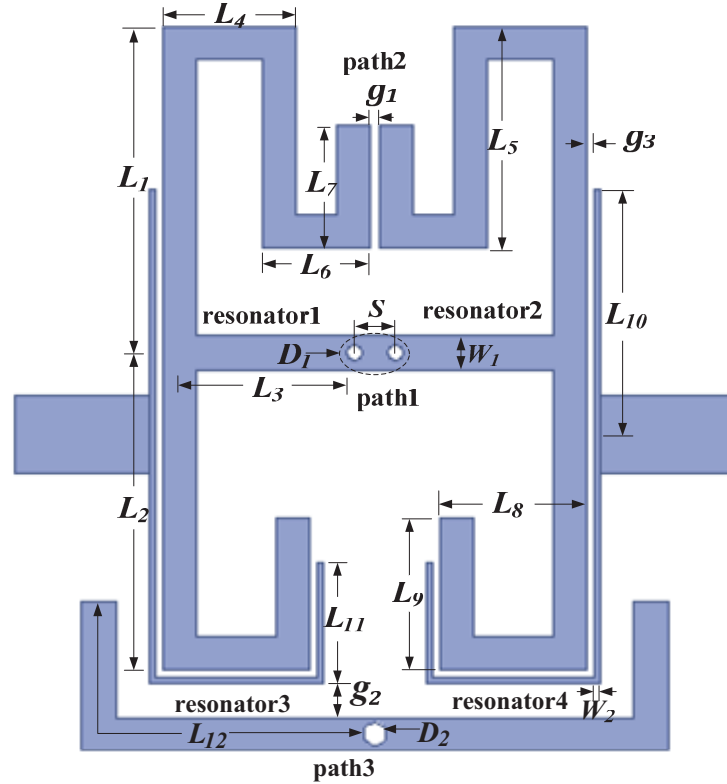
Figure 3. Configuration of the proposed tri-band bandpass filter.
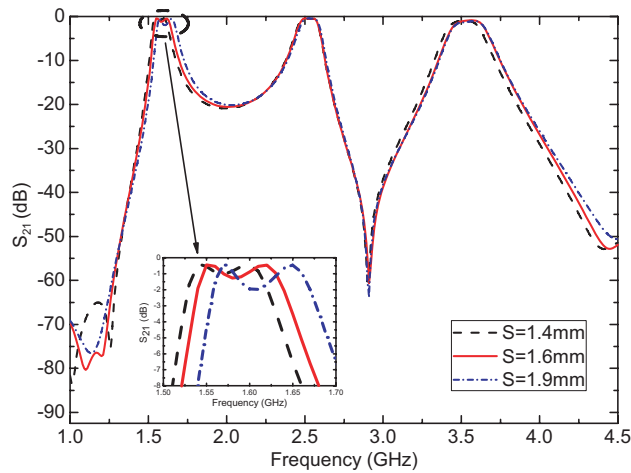
Figure 4. Relation between bandwidth and S shown in Fig. 3 in path 1.
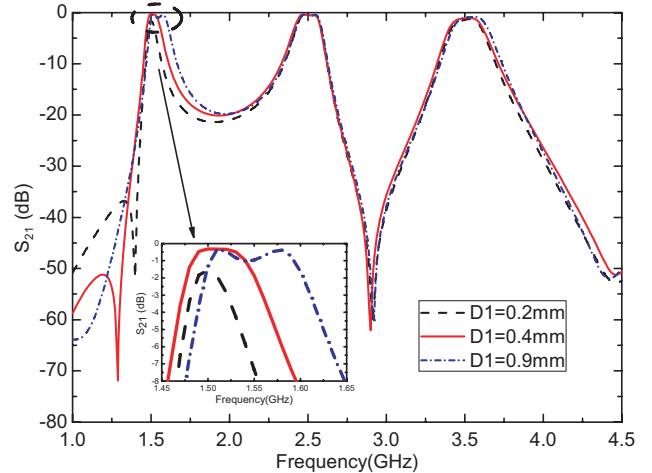
Figure 5. Relation between bandwidth and D_1 shown in Fig. 3 in path 1.

2.2.3. The Coupling of Path3

Figure 7 shows that bandwidth of the third passband can be controlled by changing distance D_2. With the decrease of D_2, the coupling effect between two uniform impedance resonators will be stronger which leads to a wider bandwidth.

Hence, coupling of the first passband is mainly affected by *path1* and *path2*. Coupling of the harmonic passband is mainly affected by *path2*. Coupling of the third passband is controlled by *path3* independently.
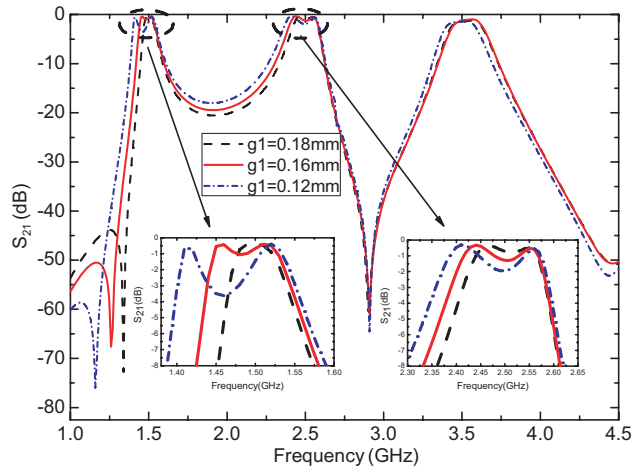
Figure 6. Relation between bandwidth and g_1 shown in Fig. 3 in path 2.
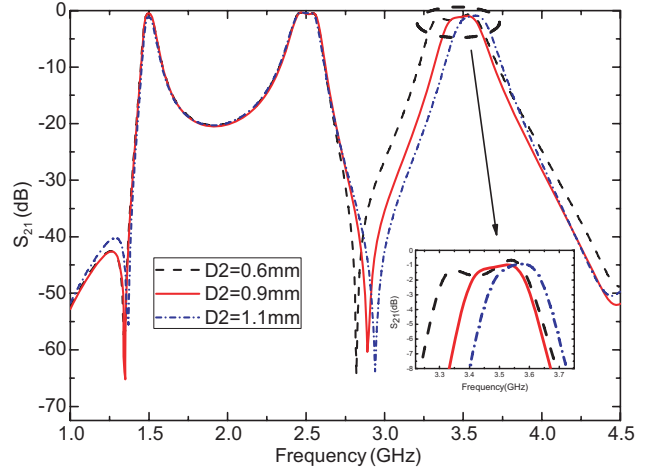
Figure 7. Relation between bandwidth and D_2 shown in Fig. 3 in path 3.

Therefore, in the design procedure, we can first determine the dimension of *path2* which affects bandwidth of the harmonic passband, then, adjust the dimension of *path1* to obtain the required bandwidth at the first passband without affecting the harmonic passband; finally, *path3* can be tuned to control the bandwidth of the third passband, without affecting the first passband and harmonic passband. So the harmonic passband can be adjusted separately and is independent of the fundamental passband. As a result, three different coupling paths are employed to control the three passbands' bandwidths, which forms a fundamental passband and harmonic passband independently controllable passband filter.

2.3. External Quality Factors

The feed circuit shown in Fig. 3 is a combination of conventional tap coupled-line and parallel coupled-line, which divide stub-loaded resonators and $\lambda/4$ resonators.

The external quality factors is determined by the coupling between the feed lines and resonators. Small coupling gaps result in large Q_e at the three passbands. For coupling gaps, g_2 is the gap between $\lambda/4$ resonators and parallel coupled-line feed which mainly affects Q_e at the third passbands; g_3 is the gap between $\lambda/4$ resonators and parallel coupled-line feed which affects Q_e at both the first and second passbands.

We next present the relations between the feed lines and bandwidths of each passband. The simulated results are shown in Fig. 8, Fig. 9.

3. RESULTS AND DISCUSSION

To verify the proposed scheme, a tri-band bandpass filter is designed, fabricated and tested. The layout of the filter is shown in Fig. 3. The three center frequencies are specified at 1.5 GHz, 2.5 GHz, and 3.5 GHz, respectively. The corresponding 3 dB fractional bandwidths (FBWs) are set as 5%, 7%, and 6%, respectively. The substrate has a relative permittivity of 2.65 and loss tangent of 0.0009. The thickness of the substrate is 1.0 mm.

To meet the first and second center frequencies, we map them to normalized frequencies as $k_1 = 1.5/1.76 = 0.85$ and $k_2 = 2.5/1.76 = 1.42$. Then, we can explicitly determine that the electrical lengths are $\theta_1 = 78°$, $\theta_2 = 57°$, and $\theta_3 = 17°$ from Eq. (2) and Fig. 1, and the corresponding geometry lengths are 22.68 mm, 16.57 mm, and 4.94 mm, respectively.

According to Eq. (3), length of the quarter-wavelength uniform impedance resonator is $L_{12} = 13.16$ mm. To obtain required three bandwidths, we employ a full-wave electromagnetic simulation method to analyze and optimize geometric parameters of the tri-band filter.
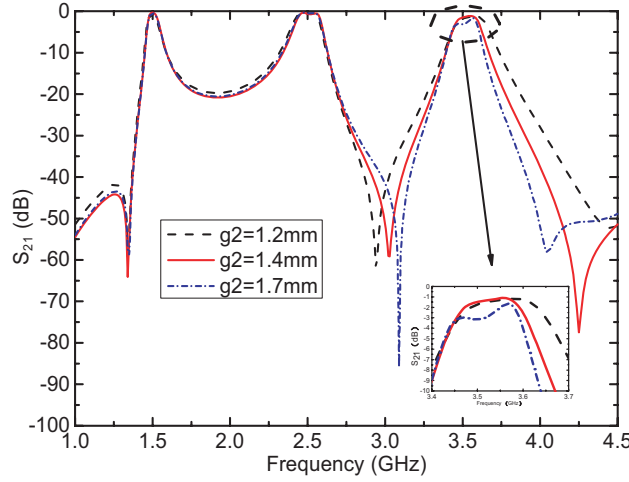
Figure 8. Relation between bandwidth and coupling gap g_2 shown in Fig. 3 in feed line.
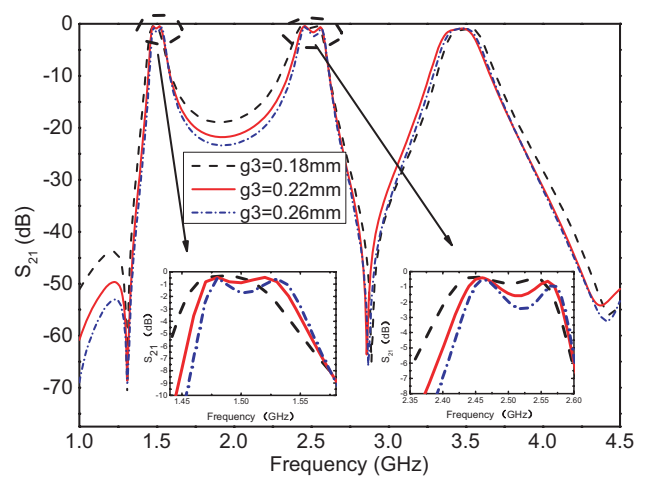
Figure 9. Relation between bandwidth and coupling gap g_3 shown in Fig. 3 in feed line.
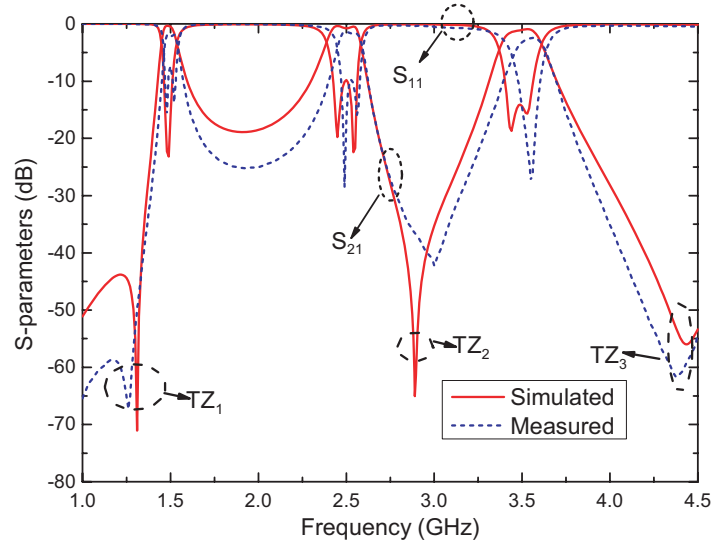
Figure 10. Simulated and measured S-parameters of the filter shown in Fig. 3 ($L_1 = 10$, $L_2 = 10.5$, $L_3 = 6.105$, $L_4 = 3.746$, $L_5 = 6.5$, $L_6 = 2.54$, $L_7 = 3.1$, $L_8 = 3.9$, $L_9 = 4.1$, $L_{10} = 8.7$, $L_{11} = 4$, $L_{12} = 3.51$, $W_1 = 1.17$, $W_2 = 0.25$, $D_1 = 0.25$, $D_2 = 0.95$, $S = 0.55$, $g_1 = 0.188$, $g_3 = 0.18$, $g_2 = 1.2$), respectively. (all are in mm).

The stub lengths obtained from the optimization are $L_1 + L_4 + L_5 + L_6 + L_7 = 25.89$ mm, $L_2 + L_8 + L_9 = 18.5$ mm, and $L_3 = 6.105$ mm, respectively. They are a litter larger than the analysis results, which may be due to the discontinuity effect of microstrip lines. The simulated response curve for the filter is plotted in Fig. 10. As can be seen, the first passband ranges from 1.449 GHz to 1.535 GHz with a 3 dB FBW of 5.76%; the second passband ranges from 2.39 GHz to 2.58 GHz with a 3 dB FBW of 7.65%; the third passband ranges from 3.39 GHz to 3.603 GHz with a 3 dB FBW of 6.09%. Minimum insertion losses for the three passbands are 0.34 dB, 0.76 dB, and 1.08 dB, respectively, and return losses are 12.5 dB, 10.1 dB, 14.3 dB, respectively. Three TZs (TZ$_1$-TZ$_3$) are generated at 1.31, 2.89, and 4.42 GHz, resulting from inherent characteristics of resonators and the couplings among resonators. Table 1 shows some reported performance of triple-band bandpass filters in recent years for comparison.

To test the proposed filter, we fabricate a filter sample, which is shown in Fig. 11. The whole size

Table 1. Performance comparison between the proposed filter and other techniques.

	1st/2nd/3rd Passbands (GHz)	S_{11} (dB)	S_{21} (dB)	3 dB FBW (%)	Circuit size $(\lambda_g * \lambda_g)$	A/B
[4]	2.4/3.5/5.45	1.1/1.2/1	15/15/15	11.6/6.7/17.8	0.21 * 0.11	Yes/Yes
[5]	3.48/4.18/5.52	1.53/2.11/2.65	15.1/22.8/19	7/5/6	0.35 * 0.17	Yes/No
[7]	2.4/3.5/5.2	1.4/1.1/1.7	18/11/20	7.5/11.7/4.03	0.23 * 0.19	Yes/No
[8]	1.84/2.45/2.98	0.9/1.6/0.8	20/15/15	4.9/3.5/5.7	0.22 * 0.27	Yes/No
[11]	2.4/3.5/5.7	0.7/1.9/0.9	12/19/12	13.6/3.68/9.87	0.28 * 0.23	Yes/No
Proposed filter	1.49/2.49/3.50	0.34/0.76/1.08	12.5/10.1/14.3	5.76/7.65/6.09	0.202 * 0.26	Yes/Yes

λ_g is the guided wavelength at the center frequency of the first passband in the free space. Lable A stands for the independent control of passband locations. While lable B stands for the independent control of passband bandwidths of the three passbands.

(a)   (b)
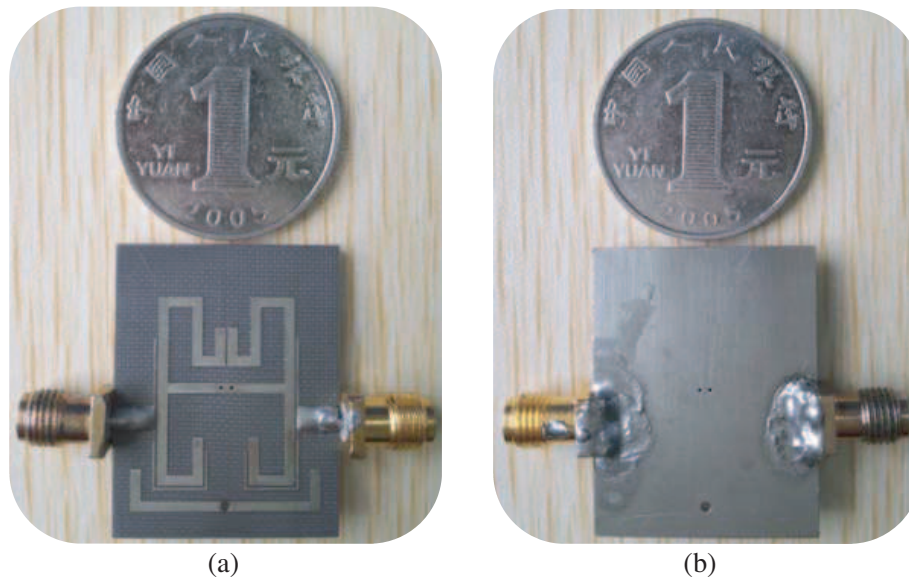
Figure 11. Photograph of the filter sample. (a) Top view. (b) Bottom view.

of the filter is 24.8 mm × 32 mm, about $0.202\lambda_g \times 0.260\lambda_g$ (λ_g is the guided wavelength at the center frequency of the first passband). The measured results are also plotted in Fig. 8 for comparison with the simulated ones. We can see that the agreement is quite good except a small frequency shift. The discrepancy may be caused by fabrication errors and deviations of material properties.

4. CONCLUSION

A compact tri-band BPF with controllable bandwidths is presented. Two grounded vias are utilized to realize coupling to obtain a coupling path. Three different coupling paths are independently exploited to control the coupling effect and bandwidth of each passband. Therefore, both the frequency and bandwidth of each passband can be designed and tuned easily, and the harmonic passband can be adjusted separately and is independent of the fundamental passband. As a result, a fundamental passband and harmonic passband independently controllable passband filter is formed. The filter has been designed, fabricated, and measured with insertion losses of 0.34, 0.76 and 1.08 dB.

REFERENCES

1. Chu, Q. X., X. H. Wu, and F. C. Chen, "Novel compact tri-band bandpass filter with controllable bandwidths," *IEEE Microwave and Wireless Components Letters*, Vol. 21, No. 12, 655–657, 2011.

2. Liang, J. G., C. Wang, and N. Y. Kim, "Compact and highly selective dual/tri-band BPFs using folded T-shaped stub-loaded resonators for WLAN and WiMAX applications," *Microwave and Optical Technology Letters*, Vol. 58, No. 2, 312–319, 2016.

3. Zhang, X. Y., C. H. Chan, Q. Xue, and B. J. Hu, "Dual-band bandpass filter with controllable bandwidths using two coupling paths," *IEEE Microwave and Wireless Components Letters*, Vol. 20, No. 11, 616–618, 2010.

4. Gao, L., X. Y. Zhang, and Q. Xue, "Compact tri-band bandpass filter using novel eight-mode resonator for 5G WiFi application," *IEEE Microwave and Wireless Components Letters*, Vol. 25, No. 10, 660–662, 2015.

5. Mo, Y., K. Song, and Y. Fan, "Miniaturized triple-band bandpass filter using coupled lines and grounded stepped impedance resonators," *IEEE Microwave and Wireless Components Letters*, Vol. 24, No. 5, 333–335, 2014.

6. Chen, F.-C., J.-M. Qiu, H.-T. Hu, and Q.-X. Chu, "Triband bandpass filter using asymmetrically loaded resonators," *Microwave and Optical Technology Letters*, Vol. 56, No. 8, 1862–1865, 2014.

7. Chu, Q. X., F. C. Chen, Z. H. Tu, and H. Wang, "A novel crossed resonator and its applications to bandpass filters," *IEEE Transactions on Microwave Theory and Techniques*, Vol. 57, No. 7, 1753–1759, 2009.

8. Zhang, X. Y., Q. Xue, and B. J. Hu, "Planar tri-band bandpass filter with compact size," *IEEE Microwave and Wireless Components Letters*, Vol. 20, No. 5, 262–264, 2010.

9. Chen, W.-Y., Y.-H. Su, H. Kuan, and S.-J. Chang, "Simple method to design a tri-band bandpass filter using asymmetric SIRs for GSM, WIMAX, and WLAN applications," *Microwave and Optical Technology Letters*, Vol. 53, No. 7, 1573–1576, 2011.

10. Hsu, C. I. G., C. H. Lee, and Y. H. Hsieh, "Tri-band bandpass filter with sharp passband skirts designed using tri-section SIRs," *IEEE Microwave and Wireless Components Letters*, Vol. 18, No. 1, 19–21, 2008.

11. Chen, W. Y., M. H. Weng, and S. J. Chang, "A new tri-band bandpass filter based on stub-loaded step-impedance resonator," *IEEE Microwave and Wireless Components Letters*, Vol. 22, No. 4, 179–181, 2012.

12. Wei, F., P. Y. Qin, Y. J. Guo, and X. W. Shi, "Design of multi-band bandpass filters based on stub loaded stepped-impedance resonator with defected microstrip structure," *IET Microwaves, Antennas & Propagation*, Vol. 10, No. 2, 230–236, 2016.

13. Mondal, P. and M. K. Mandal, "Design of dual-band bandpass filters using stub-loaded open-loop resonators," *IEEE Transactions on Microwave Theory and Techniques*, Vol. 56, No. 1, 150–155, 2008.